

A ROBUST BLIND DECONVOLUTION METHOD FOR NOISY IMAGES

M. Razaz and S. Nicholson

School of Information Systems,
University of East Anglia, Norwich, UK.

ABSTRACT

This paper presents a novel iterative blind deconvolution algorithm, which simultaneously generates solutions for both the PSF and the source image. The algorithm progresses by applying a priori constraints in both the Fourier and image domain to significantly reduce the size of the solution set. Within the new algorithm the image restoration is performed using the technique called Projection onto Convex Sets (POCS). The result of applying this form of non-linear restoration creates a very robust algorithm, which we call the Blind POCS Deconvolution Algorithm (BPDA). BPDA has been successfully applied to blurred and noisy synthetic and real images, it produces high quality restorations. Some of the relevant experimental results are presented and discussed.

1. INTRODUCTION

Blind deconvolution is the process of restoring an optical image without explicit knowledge of the characteristics of the imaging system. Images produced from typical confocal laser scanning or widefield optical microscopes are noisy and invariably blurred by the Point Spread Function (PSF), of the microscope system used. For correct scientific interpretation and analysis of a typical image obtained in this way, it is essential that the image is further processed to remove these aberrations. Measurement and modeling the characteristics of a microscope imaging system is not ideal and the measurements are quite difficult and time consuming to perform.

Blind deconvolution has been applied before to diverse areas such as communication, speech, spectroscopy and astronomy, see for example [9-12]. There is however only a limited amount of work in the literature which is specifically for optical microscopy applications [1,4]. Previously Razaz and Hudson developed a fast iterative non-linear blind deconvolution algorithm (BDA), which was applied to the restoration of optical microscope images [1]. This algorithm functions well when the images have high signal to noise ratio (SNR) but lacks the robustness offered by BPDA. A comparison between the two algorithms is made in the results section.

1.1 Projection Onto Convex Sets

We assume an image restoration model as in equation (1) with additive Gaussian noise distribution. This equation is ill-posed

and therefore has an infinite number of solutions, mainly due to the presence of noise. The POCS method [14] finds the source image ‘ f ’, given the observed image ‘ g ’, PSF and a number of prior constraints. Each constraint forms a closed convex set onto which a solution is orthogonally projected. For a number of constraints, the solution lies in the intersection of the corresponding convex sets. A variety of constraints can be applied.

$$g = Hf + n \quad (1)$$

The positivity constraint and the upper bound on noise are two such constraints which are represented by the closed convex sets ‘ ζ_1 ’ and ‘ ζ_2 ’ respectively, as shown in Figure 1.

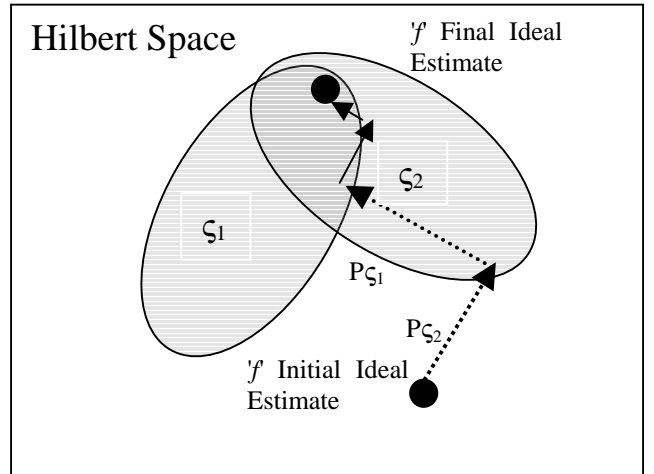


Figure 1: Shows the alternate perpendicular projections made from an arbitrary starting point in Hilbert space towards a solution of (1), which satisfies both constraints.

The distance between successive projection points shown in Figure 1, represents the change in the guess image and is termed ‘ Δf ’. The derivation of an expression for ‘ Δf ’, begins with defining the ‘norm’ of a residual vector as shown by (2).

$$\|Hf^* - g\|^2 \leq k \quad (2)$$

where

k = The upper bound on noise variance.

$$f' = f + \Delta f$$

$$r = g - Hf \quad (3)$$

Taking the upper limit of (2) and then substituting the terms from (3) into (2) results in:

$$\|H\Delta f - r\|^2 = k \quad (4)$$

This is still an ill-posed problem and must be regularised. We now introduce a regularisation procedure by modifying the 'H' operator. Modification of 'H' is made by applying constraints on the solution 'f', this condition is shown by (5), where 'c' is a constant and 'B' the regularisation operator.

$$\|Bf\| \leq c \quad (5)$$

To satisfy the two conditions proposed by (4) and (5) the two are combined and minimised with respect to the modified solution 'Δf' (6).

$$\text{Min} \left(\|H\Delta f - r\|^2 + \mu \|Bf\|^2 \right) \quad (6)$$

The solution to (6), which can be derived in various ways [14], results in the expression shown by (7) and this equation forms the basis for applying the POCS algorithm:

$$\Delta f = \frac{H^T r}{H^T H + \mu B^T B} \quad (7)$$

The 'B' matrix is often assumed to be unitary, in such cases the term $B^T B$ reduces to the identity matrix and consequently the regularisation is applied solely using the 'μ' parameter. This equation can be made computationally simpler using singular value decomposition (SVD). The SVD equivalent version to (7) is:

$$\Delta f = \frac{\sigma}{\sigma^2 + \mu} (u^T r) v \quad (8)$$

where

{ u, σ, v } represent the singular systems of 'H'.

The parameter 'μ' is known as the regularisation parameter and determines the amount of smoothing of the solution. If there is too much smoothing then the solution does not resemble the problem, if there is too little then the problems associated with using a pseudo inverse operator will be encountered. The regularisation

parameter is determined in an iterative manner using a Newton-Raphson iterative technique as in (9).

$$\mu_{k+1} = \mu_k - \frac{g(\mu_k) - k}{g'(\mu_k)} \quad (9)$$

2. THE BLIND POCS DECONVOLUTION ALGORITHM

Figure 2, shows the structure of BPDA. It is initially supplied with either a Bessel function approximation to the Point Spread Function for a microscope imaging system [7], or a theoretical PSF which takes into account certain *a priori* information about the geometry of the microscope and the chemistry of the slide [8]. Selection of either PSF's only defines the general shape of the initial PSF estimate. The size of the PSF which in turn is defined by the pixel spacing is unknown. It is estimated by finding the corresponding PSF from a set, which minimises a POCS residual measure. The technique of least squares minimisation has been utilised by other authors such as [6] using POCS and [5] using the conjugate gradient algorithm. Performing this process removes a previous necessity of BDA which was to present the algorithm with a reasonably accurate initial estimate of the PSF. The BPDA only requires that the general form of the PSF which is to be used as an initial PSF is specified. The PSF which corresponds to the smallest residual is selected as the initial PSF and is presented to the algorithm in the form of 'h₀'.

The 2D FFT is then taken to create the initial estimate of the optical transfer function (OTF), 'H₀'. The previous OTF estimate 'H_{n-1}' and the present estimate 'H_n', are then combined to form a new updated estimate of the OTF.

The first ideal image estimate in the Fourier transform domain 'F₀' is generated by restoring the observed image with POCS using the 2D IFFT of 'H₀' as the PSF. To calculate the iterated POCS restored ideal image 'F_n', the noise level of the image needs to be calculated. Once the SNR is established the SVD of the PSF is calculated. This calculation is a relatively slow process and for a 128x128 image using a magnitude only OTF it requires calculation of 65 singular systems, taking approximately four minutes of CPU time on a 180 MHz Silicon Graphics workstation. Once both of the pre-requisites are complete, POCS can perform its restoration. The restored image is combined with the previous image to form the present estimate of the ideal image 'F_n'.

The next stage in the process is to weight the present ideal image by the 'W' factor which is a Gaussian filter, this action overcomes problems encountered in extended regions of low or zero values when using inverse filters [10]. After the inverse FFT is taken of the image, the image constraints are applied.

The algorithm then performs the same steps as those described above, this time the aim is to produce the next estimate of the PSF. Once derived the PSF is constrained and is subsequently used to estimate the next ideal image. The iterations continue until the conditions for the algorithms termination are met or a predetermined number of iterations have been performed. The

termination parameter presently used is dependent upon an increase in the POCS residual measure (10):

$$residual = \|g - Hf\| \quad (10)$$

2.1 Constraints

The constraints applied to both the image and the PSF form the heart of the iterative algorithm. If no constraints are applied, execution of the BPDA will result in the deconvolved output image and PSF being the same as the initial estimates. It is therefore the case that as many effective constraints must be applied as possible. This makes the search for ‘good’ constraints intense.

By applying POCS, two constraints have already been explicitly imposed, the positivity constraint and the upper bound limit of the noise level. Other constraints which could be conditionally applied are:

- PSF spline-fitting constraint.
- PSF range and positivity.
- OTF Band-limitness constraint.
- Image spatial filtering constraint.
- Reduced set PSF constraint.

The spline fitting constraint is applied in the PSF domain, it is based on fitting a ‘bi-cubic’ spline of the best fit to the deconvolved PSF. This technique has been successfully used in the modeling of measured PSF’s [2]. The PSF can also be constrained to remove any intensity level offset and ensure that all pixel intensities are greater than or equal to zero.

The OTF band limiting constraint, limits the PSF spectrum to be of the form of a low pass filter [5], this is applied by filtering the observed image ‘G’. This ensures that the OTF, ‘ H_n ’ created by inverse filtering has attenuated values beyond the bandwidth of the imaging system. The cut-off frequency is set by the maximum resolution of the imaging system.

Literature on effective image domain constraints is sparse and has been previously limited to applying the positivity constraint [1] and conservation of image energy [10]. The BPDA however imposes spatial filtering constraints. This enhances the algorithm by combining the good qualities offered by spatial filtering noisy images using local neighbourhood statistics. One particularly effective spatial filter utilised is based on the work in [13].

Constraining the deconvolved PSF to belong to a reduced set of theoretical PSF’s generated in accordance with the work in [8], firstly ensures that all the *a priori* information available about the imaging system is used, and secondly ensures that the trivial solution to the blind deconvolution problem is avoided. The constraint is applied by selecting a PSF which minimises an error metric defined by equations (11) and (12).

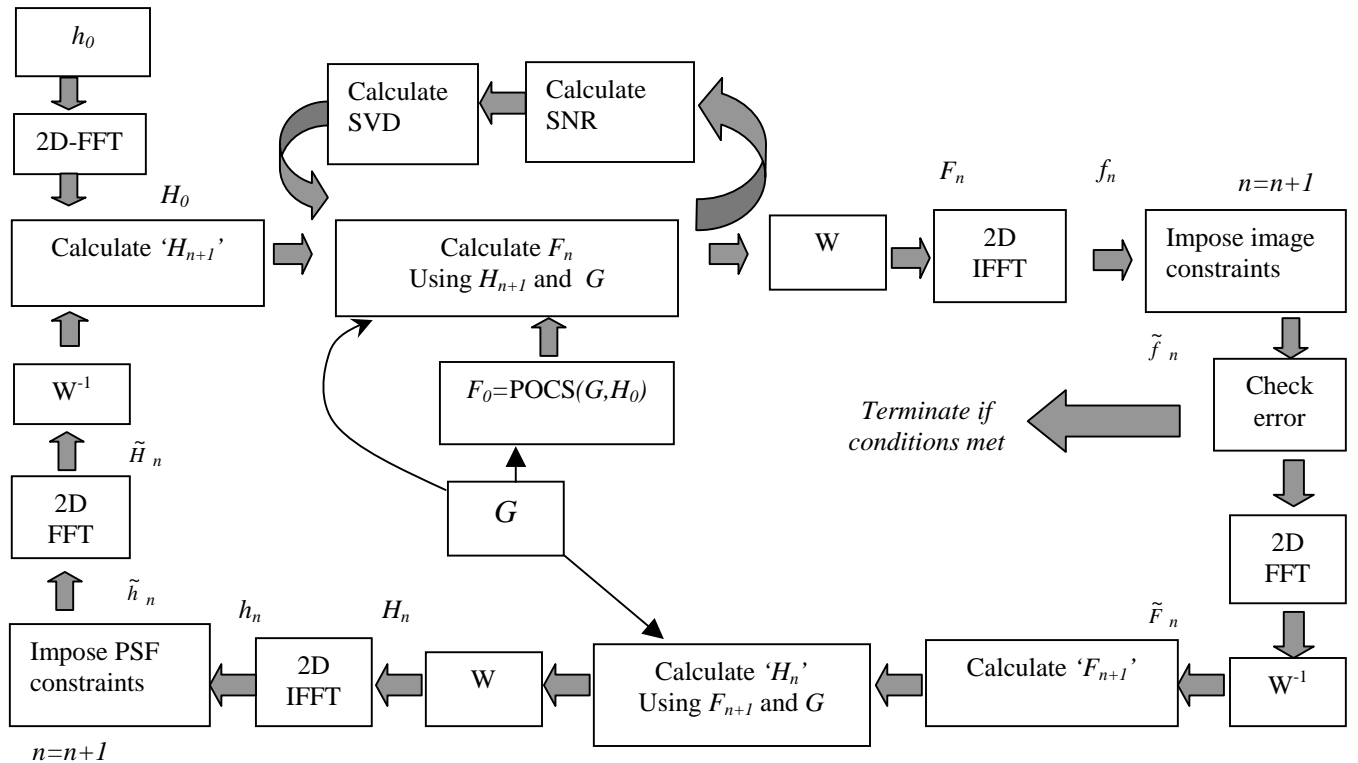


Figure 2. Block diagram of the Blind POCS Deconvolution Algorithm.

$$error = \left(\sum_{y=1}^{N_y} \sum_{x=1}^{N_x} | (h_n \circ f)_{(x,y)} - g_{(x,y)} | \right) \quad (11)$$

$$h_{ideal} = h_n(\min(error)) \quad (12)$$

For each iteration the constraint calculates the error (11) and selects the PSF ' h_n ' that corresponds to a minimum in the error function (12). This constraint when applied replaces the inverse filter used in BPDA, and thus removes all the problems associated with inverse filtering.

3. RESULTS

We have applied the new blind deconvolution algorithm BPDA to a series of synthetic and real images. We present here some typical results. All restored images shown were obtained after 6 iterations of the respective algorithms.

The image shown in Figure 3, is a 'real' image captured with a confocal microscope imaging system. The exact PSF is therefore not known. Using techniques for measuring and modeling the PSF introduced in [2], a close approximation to the true PSF can be generated. The POCS restoration using the observed image and the modeled PSF will therefore approximate the ideal or source image. This allows a quality measure to be made between the sighted restoration and the unsighted blindly deconvolved image.

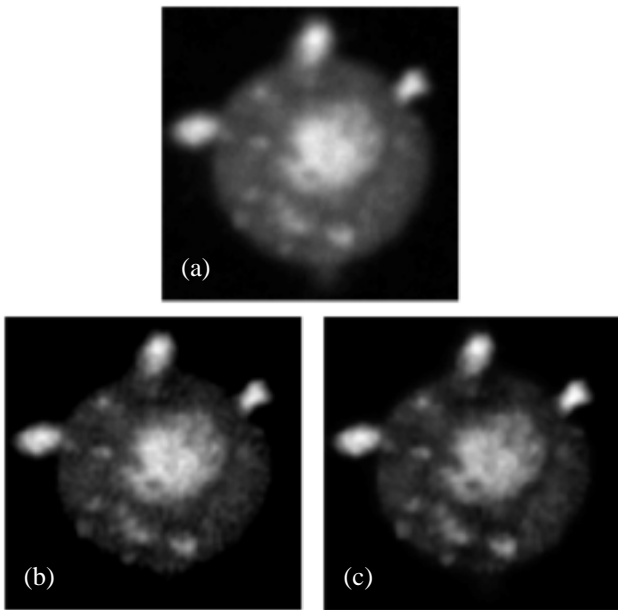


Figure 3: Restoration of a real blurred and noisy image. Figure 3a shows the original microscope image, Figure 3b shows the restoration achieved using a measured and modeled PSF and Figure 3c shows the BPDA restoration

Figure 4 shows BPDA and BDA applied to an 'artificial' image. The term artificial refers to the fact that the source image is available and is blurred by convolution with a known PSF. The blurred image is then degraded further by adding Gaussian distributed noise.

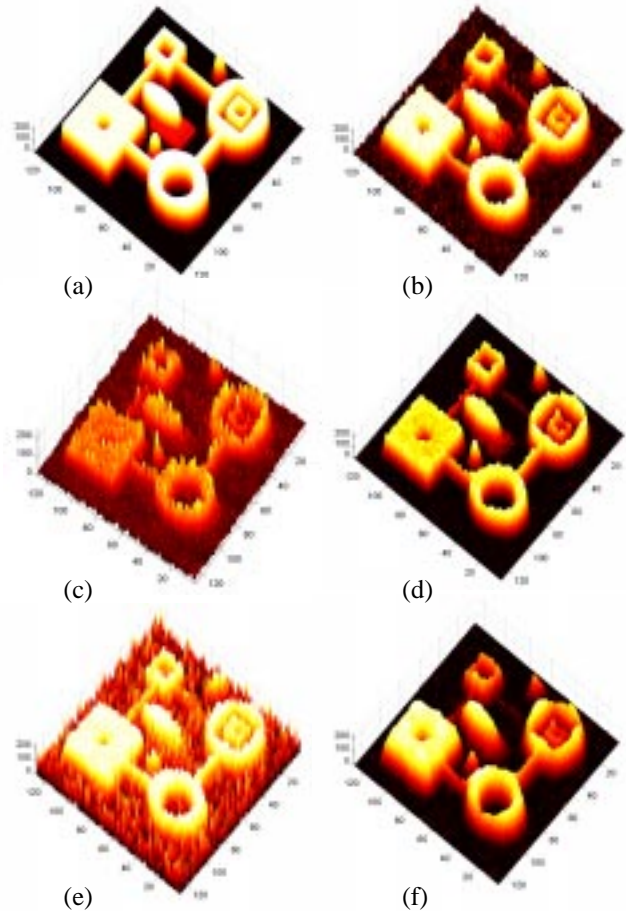


Figure 4: Blind deconvolution of a synthetic blurred and noisy image. Figure 4a shows the original image from a 3D perspective which has been chosen to highlight the noise. Figure 4b shows the blurred and noisy image (15 dB SNR). Figure 4c shows the BDA restored image and Figure 4d the restoration achieved by using BPDA. Figure 4e shows the same ideal image as Figure 4a, except that it is heavily degraded by blur and Gaussian noise (6 dB SNR). Figure 4f shows the BPDA restoration of the Figure 4e.

The final image in Figure 5 shows the BPDA restoration of an image with good SNR. The reduced PSF set constraint was applied during the blind deconvolution of this image.

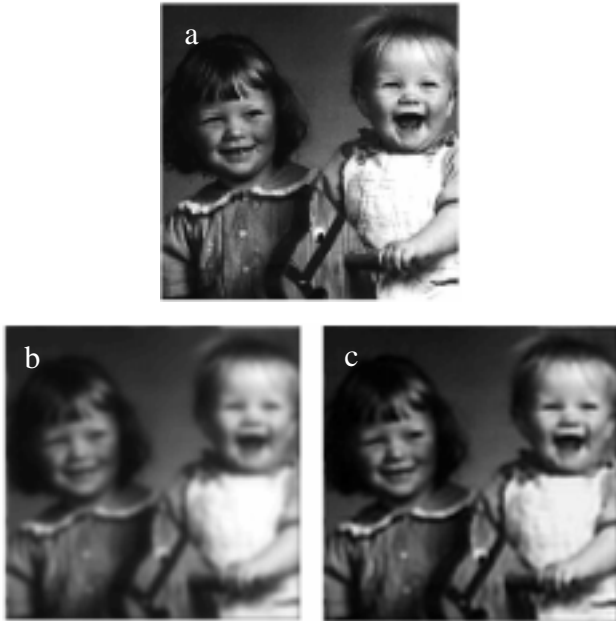


Figure 5: Blind restoration of a picture after it has been made blurred and noisy. Figure 5a shows the source image; Figure 5b shows the artificially blurred image, which has a SNR of 50 dB. Figure 5c shows the BPDA restoration.

4. SUMMARY

In this paper we presented a new iterative blind deconvolution algorithm that performs well on blurred images that have low signal to noise ratios. It has been extensively tested and the results compared to those created using BDA. For images containing moderate levels of noise the two algorithms are comparable in performance but when considerable noise is present BPDA creates far better quality restorations.

5. REFERENCES

- [1] Razaz M. and Kampmann-Hudson D., "A blind deconvolution algorithm for Image and system characterisation", *Signal processing VIII: Theories & Applications*, Vol. 2, pp. 887-890, 1996.
- [2] Razaz M., R.Lee and Shaw P.J. "Computer modeling of point spread function for 3D image restoration", *Signal Processing VII: Theories & Applications*, pp. 303-306, Sept. 1994.
- [3] Razaz M., R.Lee and Shaw P.J., "3D image restoration using a non-linear iterative deconvolution method". 3rd IMA Conf. On Math's and Signal Processing pp.10-21, Dec 1992.
- [4] Walsh T.D. and Vincent R, "Blind deconvolution of blurred images", *Electron Microscopy and Analysis*, Vol.153, pp. 191-194, 1997.
- [5] Law N.F, Lane R.G., "Blind deconvolution using least squares minimisation". *Optics Communications*, Vol. 128, pp. 341-352, 1996.
- [6] Yang Y., Galatsanos N.P. and Stark H., "Projection-Based Blind Deconvolution". *Journal of Optical Society Of America A*, Vol. 11, part 9, pp. 2401-2409, 1994.
- [7] Young I.T, "Characterising the image transfer function", in *Fluorescence Microscopy, Imaging and Spectroscopy*, Ed. D.L.Taylor and Y.L Wang, Academic Press: San Diego pp 1-45, 1989.
- [8] Hell S. , Reiner G. , Cremer C and Stelzer E.H.K, "Aberrations in confocal fluorescence microscopy induced by mismatches in refractive index", *Journal Of Microscopy*, Vol. 169, pp. 391-405, 1993.
- [9] Jefferies, S.M, Christou, J.C: " Restoration of astronomical images by iterative blind deconvolution". *The astronomical Journal*, Vol. 415, pp. 862-874, 1993.
- [10] Ayers, G.R, and Dainty, J.C, "Iterative blind deconvolution method and its applications", *Optics letters*, Vol. 13, No.7, pp. 547-549, 1988.
- [11] Jutten P. and Herault J. "Blind separation of sources", *Signal Processing*, Vol. 24, pp. 1-10, 1991.
- [12] Xu G. et al "A deterministic approach to blind channel identification", *IEEE Trans, Signal Processing*, 1995.
- [13] Lee J.S., "Digital image enhancement noise filtering by use of local statistics", *IEEE Transactions On Pattern Analysis and Machine Intelligence*, Vol. PAMI-2 pp. 165-168, 1980.
- [14] Razaz M and Lee R. A. and Shaw P. J. "Restoration of 3D real images using projection onto convex sets", *Image Processing: Math. Methods & Applic.*, Oxford Univ. Press, pp. 127-144, 1997.